Title
Influence of Strain-Rate on Localization and Strain-Softening in Normally Consolidated Clays with Varying Strength Profiles

Journal
MODELING, GEOMATERIALS, AND SITE CHARACTERIZATION (GEO-CONGRESS 2020), 2020-February(317)

ISSN
0895-0563

Authors
Oathes, Tyler J
Boulanger, Ross W

Publication Date
2020-02-21

DOI
10.1061/9780784482803.027

Peer reviewed

Influence of Strain-Rate on Localization and Strain-Softening in Normally Consolidated Clays with Varying Strength Profiles

Tyler J. Oathes, SM.ASCE[1], and Ross W. Boulanger, F.ASCE[2]

[1]Department of Civil and Environmental Engineering, University of California, Davis, 2001 Ghausi Hall, Davis CA, 95616; email: tjoathes@ucdavis.edu
[2]Department of Civil and Environmental Engineering, University of California, Davis, 2001 Ghausi Hall, Davis CA, 95616; email: rwboulanger@ucdavis.edu

ABSTRACT

The performance of geotechnical structures founded on normally consolidated (NC) clays under static or dynamic loading is dependent on the soil's strain-softening tendency and the potential for localizations to develop. Prior studies of the localization phenomenon have demonstrated that the addition of viscous (or strain-rate dependent) shearing resistance suppresses the onset of localization and provides a measure of regularization for the numerical simulation of the localization process. The onset of localization is delayed when the reduction in strength due to strain softening is counteracted by the increase in strength due to the increased strain rate that develops within a potential localization zone. Understanding localization tendencies is further complicated by spatial variability in clay properties. This paper presents a numerical study that investigates the combined effects of strain-rate, sensitivity, rate of strain softening, and varying strength profiles on the localization tendencies and the global stress-strain behavior of NC clays. The analyses were performed using the finite difference program FLAC 8.0 with the user-defined constitutive model PM4Silt modified to incorporate strain-rate effects. Parametric analyses examine the influence of strain rate, strength profile variations, local soil brittleness, and mesh size on the global post-peak stress-strain behavior of clays.

INTRODUCTION

Performing a nonlinear dynamic analysis (NDA) of a geotechnical structure founded on normally consolidated (NC) or nearly NC clay requires accounting either directly or indirectly for potential post-peak strain-softening and localization (e.g., Islam et al. 2018, Kiernan and Montgomery 2018). In practice, key issues include estimating how much deformation or strain is required during earthquake loading to fully-remold an NC or nearly NC clay or estimating how much strength reduction develops for a given level of deformation. Addressing either issue is complicated by the potential for localizations to develop in strain-softening materials, the challenge in determining appropriate localization scales (which may be on the order of mm's in an NC clay), the role of local variations in material properties (or imperfections), and the resulting mesh-dependency that arises in many numerical modeling procedures.

Authors' final copy. Published Geo-Congress 2020 GSP 317, 247-255.

The challenges in numerical modeling of strain softening and localization have long been identified. Rate-independent constitutive models have been shown to lack an internal characteristic length (e.g., Armero 1999), resulting in an inherent mesh dependency. Various schemes have been developed to address mesh dependency such as adaptive mesh refinement (Ortiz and Quigley IV 1991), dynamic relaxation (Silling 1988), and multiscale approaches (Garikipati and Hughes 2000). Rate-dependent constitutive models introduce an intrinsic length scale that reduces or eliminates the mesh-dependency of the solutions. This phenomenon, known as viscoplastic regularization, occurs when the increase in strain-rate within a developing localization zone increases the shear strength and stiffness sufficiently to reduce the ability of the shear strain and deformation to further concentrate within a single element (e.g., Niazi et al. 2013, Wang et al. 1997). Numerical simulations of a strain-rate dependent inelastic solid showed that localization occurred at approximately the same global strain regardless of the size of an imperfection in relation to the overall model (Needleman 1988), although mesh dependency still existed in the post-localization strain-softening regime. Numerical simulations with a strain-rate dependent damage model showed that the viscoplastic length scale was a function of the hardening and softening (damage) parameters and that numerical results only became mesh dependent when the effective regularization length became shorter than the element length (Niazi et al. 2013).

This paper presents a numerical study of strain softening and localization responses for a layer of rate-dependent NC clay with variable strength profiles subjected to monotonic undrained direct simple shear (DSS) loading. The critical state based, bounding surface plasticity, constitutive model PM4Silt (Boulanger and Ziotopoulou 2018, 2019) was modified to incorporate strain-rate effects and implemented as a user-defined material model in FLAC 8.0 (Itasca Consulting Group 2016). Constitutive model calibrations were developed that produce low and high rates of post-peak strain softening (or brittleness). Simulations were performed for a 1-m-thick interval having different degrees of vertical variability in the undrained shear strength parameters. Parametric studies are used to examine the influences of strain rate, strength variations, rate of strain softening (or brittleness), and mesh size on the global stress-strain and localization responses. Results are shown to be consistent with those for other types of strain-softening materials, supporting use of this modeling approach in further studies.

CONSTITUTIVE MODEL CALIBRATIONS AND STRENGTH PROFILES

The constitutive model PM4Silt was modified to incorporate strain-rate effects and implemented as a user-defined material model for use with FLAC 8.0 (Itasca Consulting Group 2016). PM4Silt (Boulanger and Ziotopoulou 2018, 2019) is a stress-ratio and critical state based, bounding surface plasticity model developed for modeling monotonic and cyclic undrained loading of clays and plastic silts. Oathes and Boulanger (2019) modified the model to incorporate a strain-rate dependent critical state line and a strain-rate dependent critical state stress ratio that are controlled by user-specified strain-rate factors based on observed or anticipated soil behavior. The strain-rate dependency is based on the Strain Rate Ratio (SRR), which is equal to the logarithm of the strain rate divided by a reference strain rate. The constitutive model has five primary and 20 secondary parameters. The five primary input parameters are (1) the critical state undrained shear strength or undrained strength ratio ($s_{u,cs}$ or $s_{u,cs}/\sigma'_{vc}$), (2) the shear modulus coefficient (G_o), (3) the contraction rate parameter (h_{po}), (4) the rate factor F_P for the critical state line dependency, and (5) the rate factor F_M for the critical state stress ratio dependency.

Two model calibrations were developed that produce the "more brittle" and "less brittle" post-peak stress-stress strain responses shown in Figure 1. These results are based upon the primary input parameters and one secondary parameter ($n^{b,wet}$) listed in Table 1. The "more brittle" calibration produces a peak strength ratio of $s_{u,pk}/\sigma'_{vc} = 0.33$ with a sensitivity of approximately 5.5 (given $s_{u,cs}/\sigma'_{vc} = 0.06$). The "less brittle" calibration produces $s_{u,pk}/\sigma'_{vc} = 0.37$ and a sensitivity of approximately 2.5 (given $s_{u,cs}/\sigma'_{vc} = 0.15$). At 10% shear strain, the shear resistances for the more and less brittle soils are about 48% and 9% smaller than their respective peak shear resistances.

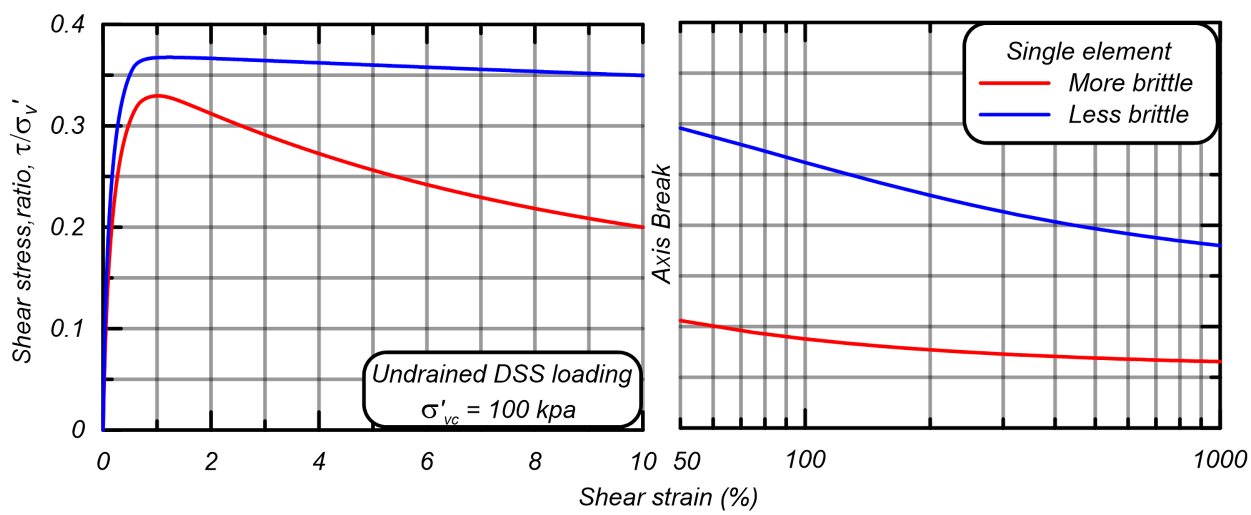

Figure 1: Single element simulations of a more and less brittle soil response to monotonic undrained direct simple shear loading

Table 1: Calibrations for the rate dependent version of PM4Silt

	Calibration No. 1: More brittle	Calibration No. 2: Less brittle
$s_{u,cs}/\sigma'_{vc}$	0.06	0.15
G_o	323	479
h_{po}	5000	15000
F_p	0.05	0.05
F_m	0.05	0.05
$n^{b,wet}$	0.1	0.1

[a] All other parameters retain default values given in Boulanger and Ziotopoulou (2018)

Profiles with vertical variability in shear strength were developed for the 1-m thick model layer by introducing random variability in the $s_{u,cs}/\sigma'_{vc}$ parameter. The variability was modeled as being normally distributed and random with a coefficient of variation (COV) of 0.0, 0.02, 0.05, and 0.10. Values of $s_{u,cs}/\sigma'_{vc}$ were generated at 4 cm spacing, and the $s_{u,cs}/\sigma'_{vc}$ profiles were up or down sampled according to the desired mesh refinement, as shown in Figure 2 for the calibration for the "more brittle" soil with a 10 element mesh. The values of $s_{u,cs}/\sigma'_{vc}$ for the "less brittle" calibration were linearly scaled from those shown in Figure 2 (i.e., multiplied by a factor of 0.15/0.06 = 2.5).

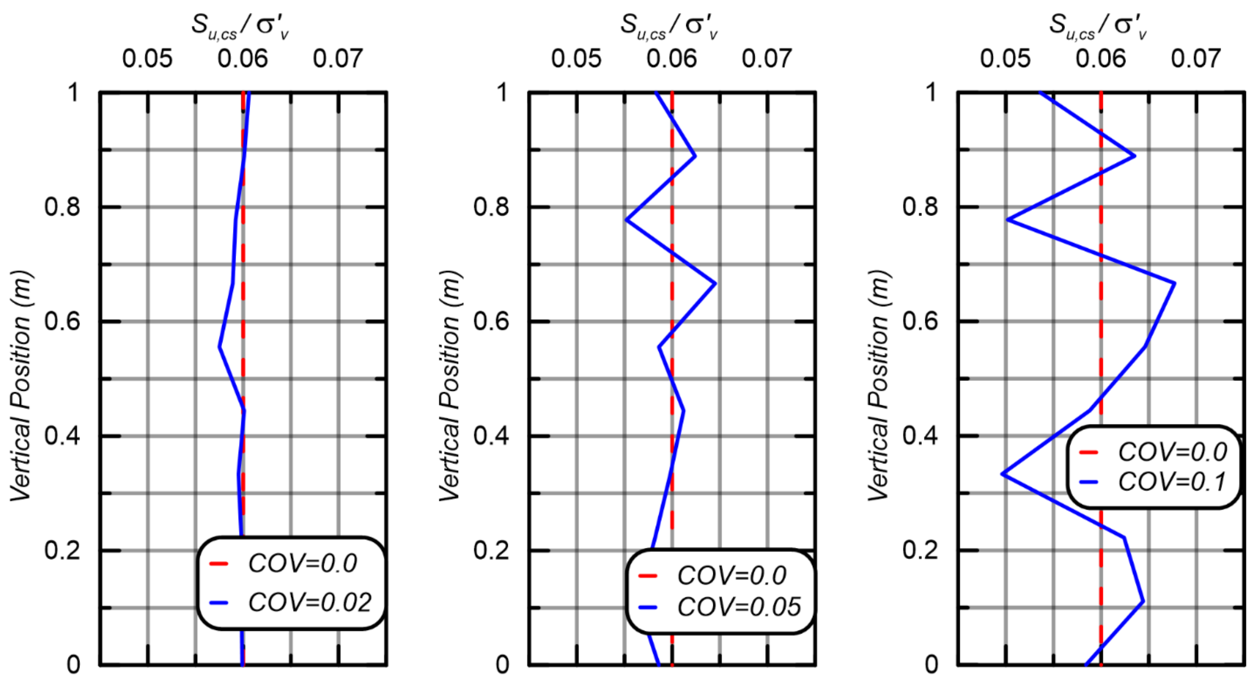

Figure 2: Profiles of $s_{u,cs}/\sigma'_{vc}$ for a 1-m thick interval based on COV of 0.02, 0.05, and 0.10 with the calibration for a "more brittle" soil.

SIMULATIONS OF UNDRAINED DSS LOADING

Simulations using single elements of undrained DSS loading were used to obtain the constitutive or local material responses to uniform strain fields. The first set of simulations using the baseline calibrations from Table 1 were presented previously in Figure 1. A second set of single-element simulations were used to obtain the local material responses for the weakest sublayer properties from each of the profiles shown in Figure 2. For the "more brittle" calibration, these cases correspond to $s_{u,cs}/\sigma'_{vc}$ values of 0.06, 0.058, 0.055, and 0.048. The variations in $s_{u,cs}/\sigma'_{vc}$ had less effect on the local material stress-strain responses at smaller strains than at larger strains for either calibration, as shown in Figure 3. The post-peak reduction in shear resistance for the less brittle calibration at 10% shear strain ranges from approximately 9% for the $COV_{su,cs}$ = 0.0 case (homogenous) to approximately 18% for the $COV_{su,cs}$ = 0.10 case. The post-peak reduction in shear resistance for the more brittle calibration at 10% shear strain ranges from approximately 48% for the homogenous case to approximately 60% for the $COV_{su,cs}$ = 0.10 case. The peak shearing resistances and the shear strain at peak shearing resistance were less affected by the variation in $s_{u,cs}/\sigma'_{vc}$.

Grid simulations of undrained DSS loading were performed using a 1-m wide by 1-m tall rectangular grid (or mesh) of soil with uniform zone (element) lengths in both directions. Different numbers of zones in each direction were used to evaluate mesh dependency of the global stress-strain responses. Stiff "caps" of elastic material were placed above and below the soil. The base was fixed in the x and y direction. The left and right sides of the model were slaved together. A uniform horizontal velocity corresponding to a global SRR of either 0 or 4 was applied to the top. The SRR = 4 with the rate factors incorporated in these analyses results in critical state strengths that are approximately 40% stronger and peak strengths that are approximately 20% stronger than obtained with SRR = 0 (compared in terms of their local material responses).

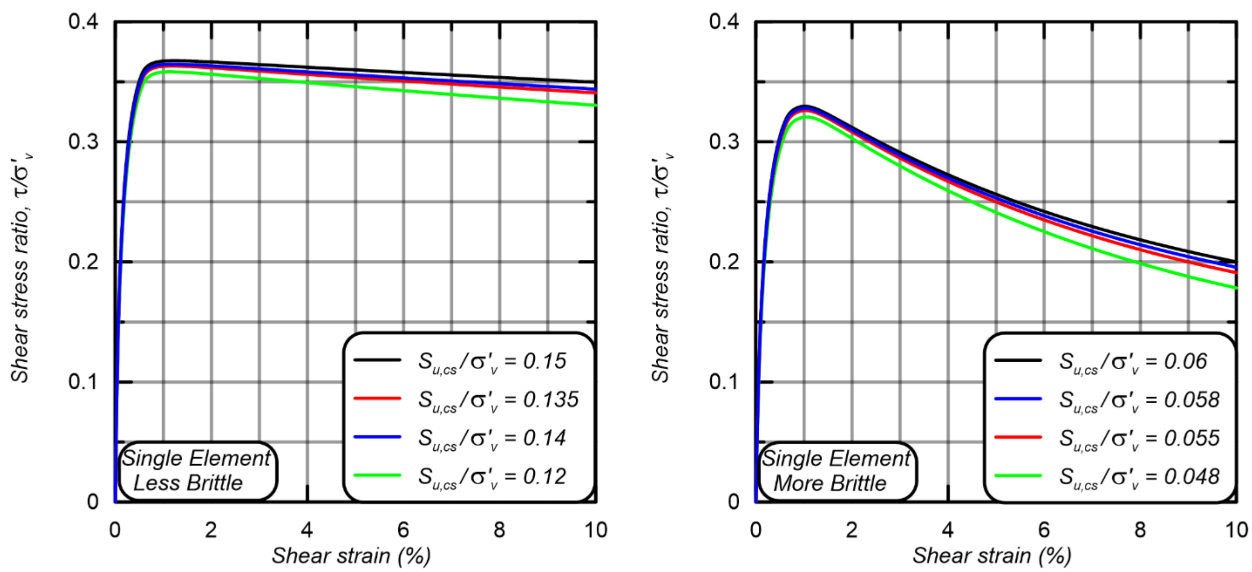

Figure 3: Single element simulations of lowest strengths in each strength profile for less brittle (left) and more brittle (right) material loaded at an SRR = 0

The effect of rate-dependent shearing resistance on localization behavior is illustrated by the global stress-strain responses shown in Figure 4 for a 10 by 10 grid with homogenous profiles of the less brittle (Figure 4a) and more brittle (Figure 4b) calibrations. Global stress-strain responses are shown for three cases: a rate independent case ($F_p = F_m = 0$), the baseline case with $F_p = F_m = 0.05$, and a case with twice the baseline rate dependence ($F_p = F_m = 0.10$). The global stress-strain responses for the strain-rate independent case shows strong post-peak strain softening for both calibrations because localizations form along a single row of zones immediately after peak shearing resistance in each simulation. The inclusion of rate dependence delays the onset of a well-defined localization until much larger shear strains; i.e., formation of well-defined localizations occurs at approximately the point where the global stress-strain curve shows a sharp increase in the rate of strain softening. The stress-strain responses are largely mesh independent until the well-defined localization forms (i.e., compare the stress-strain responses from Figures 1 and 4), after which the response becomes mesh dependent again (as discussed later). The effects of adding rate dependence to this bounding surface plasticity model are consistent with the findings by others for other types of strain softening materials (Needleman 1988, Wang et al. 1997, Niazi et al. 2013).

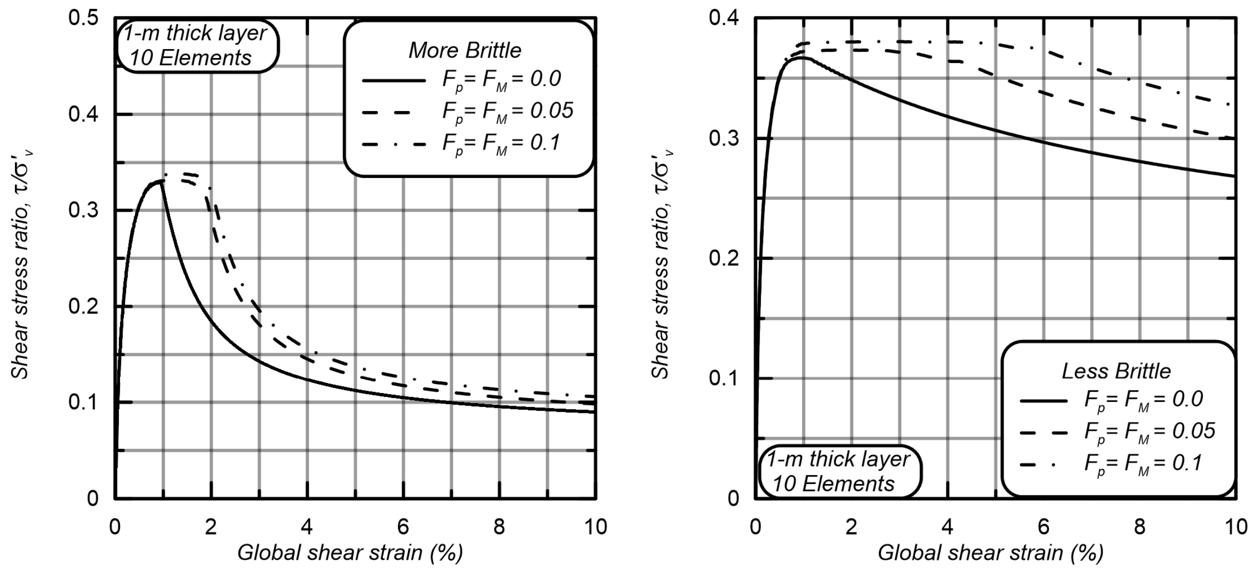

Figure 4. Effect of rate dependence on the DSS simulations using a 10 by 10 grid for SRR = 0: (a) less brittle calibration, (b) more brittle calibration.

The effect of strength variability on global stress-strain responses for the more brittle calibration is illustrated in Figure 5 for a 10 by 10 grid with the four different strength profiles loaded at an SRR of 0 (Figure 5a) and 4 (Figure 5b). For the homogenous strength profile, the global stress-strain responses show that localizations fully develop (characterized by a rapid increase in the rate of strain softening) at shear strains of approximately 1.5% and 2% for an SRR of 0 and 4 respectively (Figure 4). For the profiles based on a $COV_{su,cs} = 0.10$, localizations fully developed at shear strains of approximately 1% and 1.5% for SRR's of 0 and 4 respectively. Thus, increasing the strength variability caused a slight decrease in the shear strain at which a well-defined localization forms, as might reasonably be expected.

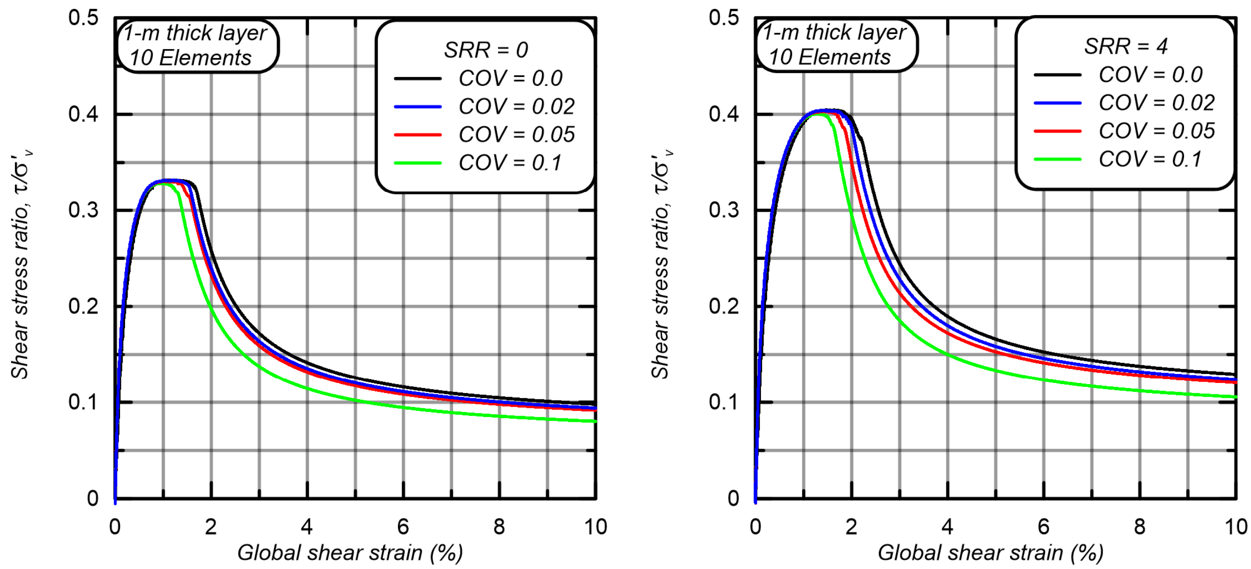

Figure 5: Results of 10 by 10 grid simulations for the more brittle soil with varying strength profiles for an SRR = 0 (left) and an SRR = 4 (right)

The effect of strength variability on the global stress-strain responses for the less brittle calibration is illustrated in Figure 6 for the same conditions as for Figure 5. For the homogenous strength profile, the global stress-strain responses show that localizations fully develop at shear strains of approximately 3.5% and 4% for an SRR of 0 and 4 respectively (Figure 6). For the profiles based on a $COV_{su,cs}$ = 0.10, localizations fully developed at shear strains of approximately 1.8% and 2% for SRR's of 0 and 4 respectively. Thus, increasing the strength variability again caused a decrease in the shear strain at which a well-defined localization forms, with the effect being larger than observed for the more brittle calibration.

The effect of strength variability on the strain at which localizations fully develop (Figures 4 and 5) appears reasonable given the mechanism by which strain rate dependence helped to delay the onset of localizations. The rate dependence used in the baseline calibrations produce about a 5% increase in peak shearing resistance per logarithmic cycle of strain rate. When the localization begins to develop, the strains begin to concentrate within the localizing element, the concentration in strains increases the strain rate by a factor equivalent to the number of elements (in this case 10), and the shearing resistance increases accordingly (by about 5% in this case) . The benefits of this rate-dependent strength increase are diminished whenever the vertical variability in strength is larger (like the case with $COV_{su,cs}$ = 0.10). Thus, the effect of strength variability depends on its magnitude relative to the potential rate dependent strength gain within the same interval.

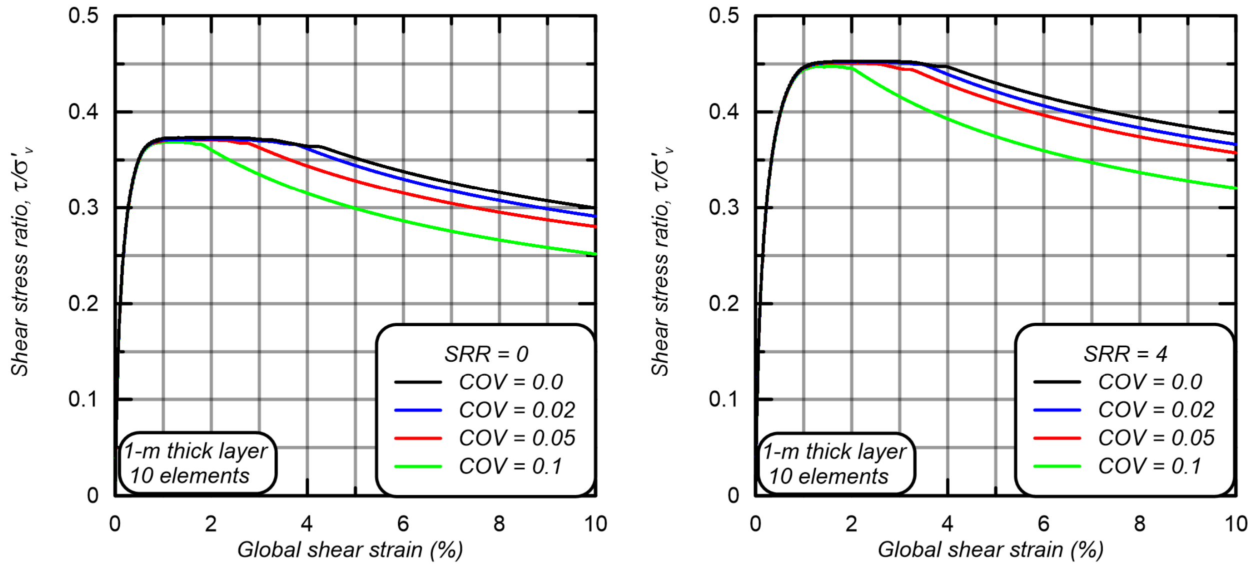

Figure 6: Results of 10 by 10 grid simulations for the less brittle soil with varying strength profiles for an SRR = 0 (left) and an SRR = 4 (right)

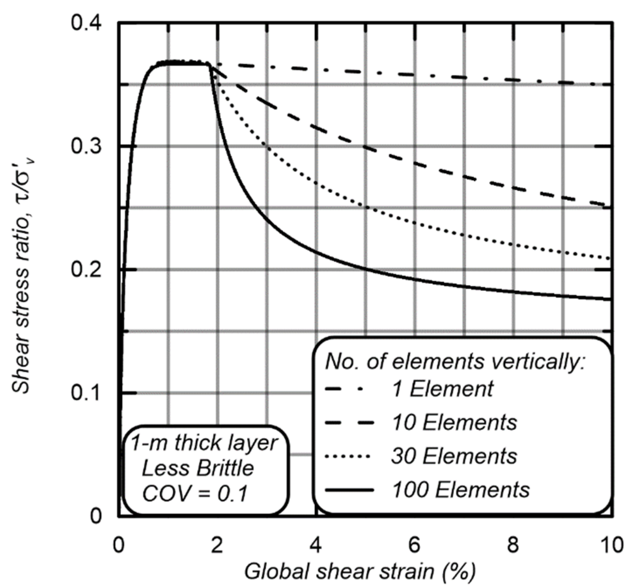

Figure 7: Results of DSS simulations with varying number of elements in vertical direction for the less brittle calibration with the $COV_{su,cs}$ = 0.1 strength profile loaded at a SRR = 0

Mesh dependence of the simulations is illustrated in Figure 7 showing the global stress-strain responses for the less brittle calibration with the $COV_{su,cs}$ = 0.1 strength profile loaded at an SRR = 0; results are shown for a single element case, a grid with 10 elements in the vertical direction, a grid with 30 elements in the vertical direction, and a grid with 100 elements in the vertical direction. Simulations using 10, 20, 30, or 100 elements in the horizontal direction showed that results were insensitive to the element aspect ratio. The minimum thickness of a localization zone is the height of a single element, or about 100 cm, 10 cm, 3.3 cm, and 1 cm for the grids used to produce Figure 7. The various grid simulations approximately follow the single element simulation response during the initial phase of strain-softening (from a shear strain of about 1% to a shear strain of about 2%), which is indicative of the intrinsic length scale and regularization introduced by the strain-rate dependence for this baseline calibration. After a localization has fully developed (at a shear strain of about 2%), the solution again becomes mesh dependent with the rate of strain-softening increasing with an increasing number of elements due to the more rapid accumulation of shear strain within a thinner localization zone. The responses observed in Figure 7 are consistent with those seen in in numerical simulations of other strain-rate dependent, strain-softening materials (Needleman 1988, Wang et al. 1997, Niazi et al. 2013).

CONCLUSION

Evaluating the performance of geotechnical structures founded on NC or nearly NC clays under static or dynamic loading requires assessing the soil's strain-softening behavior and the potential for localizations to develop. Studies of localization phenomena in other strain-softening materials have shown that accounting for strain-rate dependence of the shearing resistance can delay the onset of localization and provide a measure of regularization for numerical simulations. The onset of localization can be delayed when the reduction in shearing resistance due to strain softening within a potential localization zone is counteracted by an increase in shearing resistance due to the increased strain rate within the potential localization zone.

A numerical study of strain softening and localization responses was presented for a 1-m-thick layer of strain rate-dependent NC clay subjected to monotonic undrained direct simple shear (DSS) loading. The critical state based, bounding surface plasticity constitutive model PM4Silt (Boulanger and Ziotopoulou 2018, 2019) was modified to incorporate strain-rate effects and used with FLAC 8.0 (Itasca Consulting Group 2016) to perform the simulations. The results of parametric analyses illustrated how the global stress-strain response and localization phenomena were affected by the strain rate, the post-peak strain-softening rate (or brittleness), strength variations within the layer, and mesh size. The inclusion of rate dependent shearing resistance was shown to delay the onset of localization and provide a measure of regularization (mesh independence) until a localization fully developed, consistent with the results of prior studies for other types of strain-softening materials. These initial results provide support for using this modeling approach in future studies of strain softening and localization in soft clays.

ACKNOWLEDGEMENTS

The work described herein was funded by the California Department of Water Resources under Contract 4600009751. Any opinions, findings, or recommendations expressed herein are those of the authors and do not necessarily represent the views of this organization. The authors appreciate the above support.

REFERENCES

Armero, F. (1999). “Large-scale modeling of localized dissipative mechanisms in a local continuum: Applications to the numerical simulation of strain localization in rate-dependent inelastic solids.” Mechanics of Cohesive-Frictional Materials, 4(2), 101–131.

Boulanger, R. W., and Ziotopoulou, K. (2018). “PM4 Silt (Version 1): A silt plasticity model for earthquake engineering applications.” Report No. UCD/CGM-18-01, Center for Geotehcnical Modeling, Department of Civil and Environmental Engineering, University of California, Davis, Ca, 108 pp.

Boulanger, R. W., and Ziotopoulou, K. (2019). "A constitutive model for clays and plastic silts in plane-strain earthquake engineering applications." Soil Dynamics and Earthquake Engineering, 127(2019): 105832, 10.1016/j.soildyn.2019.105832.

Garikipati, K., and Hughes, T. J. R. (2000). “Variational multiscale approach to strain localization - formulation for multidimensional problems.” Computer Methods in Applied Mechanics and Engineering, 188, 39-60

Islam, N., Hawlader, B., Wang, C., and Soga, K. (2018). "Large-deformation finite-element modelling of earthquake-induced landslides considering strain-softening behaviour of sensitive clay." Canadian Geotechnical Journal, 56: 1003–1018 (2019) dx.doi.org/10.1139/cgj-2018-0250.

Itasca Consulting Group, I. (2016). “FLAC - Fast Lagrangian Analysis of Continua, Ver 8.0.” *Minneapolis*, 1–6.

Kiernan, M., and Montgomery, J. (2018). “Numerical Simulations of the Fourth Avenue Landslide Considering Strain-Softening.” Proc., Geotechnical Earthquake Engineering and Soil Dynamics V,Geotechnical Special Publication 290, S.J. Brandenberg and M.T. Manzari,eds., ASCE, 67–78.

Needleman, A. (1988). “Material rate dependence and mesh sensitivity in localization problems.” Computer Methods in Applied Mechanics and Engineering., 67, 69-85.

Niazi, M. S., Wisselink, H. H., and Meinders, T. (2013). “Viscoplastic regularization of local damage models: Revisited.” *Computational Mechanics*, 51(2), 203–216.

Oathes, T. J., and Boulanger, R. W. (2019). “Numerical Evaluation of Strain-Rate Effects on Strain-Softening and Localization in Saturated Clays.” Proc., Second City - Second Chances: Stories of Rehabilitation, Modification, and Reviatalization, 39th USSD Annual Meeting and Conference, United States Society of Dams, Chicago, IL, 1–15.

Ortiz, M., and Quigley IV, J. J. (1991). “Adaptive mesh refinement in strain localization problems.” Computer Methods in Applied Mechanics and Engineering., 90, 781-804.

Silling, S. A. (1988). “Finite difference modeling of phase changes and localization in elasticity.” Computer Methods in Applied Mechanics and Engineering., 70, 251-273.